SAN-1459-3

Technical Progress Report No. 3

30 June 1978

Period 1 March 1978 - 31 May 1978

LMSC-D626523

CADMIUM SULFIDE/COPPER SULFIDE HETEROJUNCTION CELL RESEARCH

Contract No. EG-77-C-03-1459

Electro-Optics Laboratory
Electronics and Communication Sciences
Lockheed Palo Alto Research Laboratory
LOCKHEED MISSILES & SPACE COMPANY, INC.
Palo Alto, California 94304

DISCLAIMER

This report was prepared as an account of work sponsored by an agency of the United States Government. Neither the United States Government nor any agency thereof, nor any of their employees, makes any warranty, express or implied, or assumes any legal liability or responsibility for the accuracy, completeness, or usefulness of any information, apparatus, product, or process disclosed, or represents that its use would not infringe privately owned rights. Reference herein to any specific commercial product, process, or service by trade name, trademark, manufacturer, or otherwise does not necessarily constitute or imply its endorsement, recommendation, or favoring by the United States Government or any agency thereof. The views and opinions of authors expressed herein do not necessarily state or reflect those of the United States Government or any agency thereof.

DISCLAIMER

Portions of this document may be illegible in electronic image products. Images are produced from the best available original document.

INTRODUCTION - SUMMARY

The program objective is to investigate and evaluate the application of cylindrical-post magnetron reactive sputtering to the production of solar cell quality thin films of CdS/Cu_2S for large scale terrestrial photovoltaic energy conversion.

The primary activities during the third quarter reporting period were directed toward the following tasks:

- Assembly of Specialized Deposition System (Task 1.1)
- Deposition of $Cd_{1-x}Zn_xS$ (Task 1.2)
- Substrate Contact (Task 1.3)
- Deposition of Cu_2S (Task 1.6)
- Electrical Measurements of Cu_xS (Task 1.8)
- Structural Measurements of Cu_xS (Task 1.7)

There has been a lower than anticipated rate of spending and activity through the third quarter period due to continued delays in delivery of high purity sputtering targets from the vendor. Fabrication of all parts for the specialized deposition apparatus, with the exception of the sputtering targets, has been completed. The only remaining task is to shakedown the system.

Cominco American has encountered difficulties in maintaining the desired 6-9's purity while casting Cd, Cd-Zn, and Zn sputtering targets over the nickelplated copper mandrels which are used to provide strength to the overall assembly. Therefore, it is anticipated that there will be an additional delay before the high purity targets are available. Thus a reject Cd target assembly with approximately 5-9's purity, that was cast during a first attempt at fabricating the high purity targets, has been purchased from Cominco American and is being used to conduct certain aspects of the CdS reactive sputtering studies. It is anticipated that a Cd-20 atomic percent Zn cathode of similar purity will also be procured for use in the interim prior to delivery of the high purity targets.

A major activity during the third quarter reporting period has been a systematic study of Cu_xS coatings deposited by reactive sputtering Cu in Ar-H_2S gas mixtures at various injection rates (partial pressures) of H_2S. The coatings were deposited on borosilicate glass substrates at substrate temperatures of about 35° C and 130° C. The coatings were analyzed with respect to electrical, optical, and structural characteristics. Van der Pauw and temperature dependence of resistivity measurements were made on selected films. Optical constants were obtained from transmission and reflection measurements. Structural and compositional measurements were made using x-ray diffraction, scanning electron microscopy, microprobe, and x-ray energy spectroscopy.

For H_2S partial pressures greater than 1.4 mtorr, we have found that two types of Cu_xS films, i.e., high resistivity and low resistivity, can be deposited on glass substrates using T_s as the primary control parameter. Generally, the high resistivity films contain Cu-rich nodules which appear to be growing out of the film. Both chalcocite and djurleite phases are present in some films, with djurleite predominant in the low resistivity films.

TECHNICAL DISCUSSION

Assembly of Specialized Deposition System (Task 1.1)

The specialized deposition system is designed to locate four magnetron sputtering sources surrounding a rotatable substrate holder, as shown in Figure 1. Thus the apparatus permits multi-layer coatings of various configurations to be deposited without breaking vacuum. Preliminary material studies are being made with the apparatus configuration shown in Figure 2. This configuration places two substrate holders around a single magnetron source having shields to simulate the situation in the multi-cathode apparatus. The fabrication of all elements for the specialized deposition system - i.e., the chamber mounting plate, the magnetron sputtering sources, and the rotatable substrate holder - have been completed. However, all deposition work thus far has been with the single source configuration shown in Figure 2. Thus the final installation and shakedown of the multi-cathode apparatus remains to be done. This installation has been delayed because the configuration shown in Figure 2 permits a larger number of substrates to be coated during a given deposition run. However, it is anticipated that the multi-cathode apparatus will be placed in operation soon, so that the CdS/Cu_2S junction studies can begin.

It was noted in Technical Progress Report Number 2 that some regulator malfunctioning in the form of a pulsing gas flow had been observed in the H_2S gas injection system. These problems appear to have been solved by rebuilding the Matheson two-stage regulator (Type 3800) with the operating pressures of the two stages carefully adjusted for service with the pressure provided by the H_2S supply tank (the vapor pressure over liquid H_2S at room temperature, i.e. ~ 250 psig). In addition, a Varian type 951-5106 variable leak valve has been procured to improve the adjustment control over the H_2S injection rate.

An H_2S scrubber has been fabricated and added to the exhaust line of the vacuum chamber pumping system. The scrubber consists of a vertically mounted 3-inch diameter pyrex pipe which is filled with a 1-molar solution

of NaOH and water. The pump exhaust passes through a stainless steel porous plug at the bottom of the pipe and up through the pipe, where it undergoes the reaction:

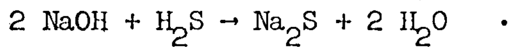

$$2\ NaOH + H_2S \rightarrow Na_2S + 2\ H_2O \quad .$$

The scrubber appears to be functioning adequately. When approximately 40 scc/min of H_2S was passed through the scrubber, no H_2S could be detected by smell at the output (one can detect about 2-3 ppm H_2S by smell).

A Brush type 260 five-channel strip chart recorder is being added to the deposition system. It is planned that the substrate temperatures, discharge voltage, total gas pressure, and reactive gas flow rate will be monitored.

Deposition of $Cd_{1-x}Zn_xS$ (Task 1.2)

Target Fabrication Problem

Progress in the $Cd_{1-x}Zn_xS$ deposition studies has been delayed by difficulties encountered in fabricating the high purity sputtering targets. A cylindrical magnetron sputtering target consists of a tube and end discs, as shown in Figure 1 of Technical Progress Report Number 2. In preliminary studies conducted at Telic prior to initiation of the present program, a Cd sputtering target was formed by casting 6-9's pure Cd over a mandrel and end discs fabricated from type 304 stainless steel. The stainless steel was used to give strength to the overall assembly. The purity of the final casting was not tested. It was decided at the beginning of the present program that a similar procedure would be used, but that the support forms would be made from Cu, to provide better thermal conductivity, and electroplated with Ni to provide a diffusion barrier. Cominco American of Spokane, Washington, was selected to perform the casting.

Cominco American cast 6-9's Cd, Cd - 10 atomic percent Zn, Cd - 20 atomic percent Zn, and Zn over Ni-plated Cu mandrels supplied by Telic. The casting was done in a propane atmosphere at a temperature just slightly above the

LOCKHEED PALO ALTO RESEARCH LABORATORY
LOCKHEED MISSILES & SPACE COMPANY, INC.
A SUBSIDIARY OF LOCKHEED AIRCRAFT CORPORATION

melting point. The freezing time is estimated to have been from 2 to 5 min. No obvious problems were noted in the casting. However, when an attempt was made to cast Cd on the first set of end discs, poor wetting to the Ni was noted. Therefore, the Ni was given a light etch to remove the oxide, and the temperature of the molten Cd was raised slightly. During casting there was visual evidence of localized buckling failures within the Ni layer, probably resulting from gas which was trapped in the Ni coating during electroplating. At this point we asked Cominco American to examine the targets carefully for evidence of impurities. A test section was cut from the Cd tube and examined by emission spectroscopy. The tubes were cast with a Cd wall thickness of about twice the 1/4" requested by Telic. Thus a section of the Cd tube was machined down to the desired thickness, and an analysis was made of the composition of the surface. A contamination level of 20 ppm Ni and 3 ppm Cu was detected in two tests. The Cd was then machined down to a wall thickness of 1/8". The same contamination level was detected in two additional samplings. A similar test was conducted on the Cd end discs after machining the casting down to the size specified by Telic. The top end disc yielded 40 ppm Cu and 10 ppm Ni, and the bottom disc yielded 100 pm Cu and 20 ppm Ni. All other contaminants were within the 6-9's specification in all of the tests.

A 5-9's purity level should be adequate for the Zn target, since this is used simply to form an anti-reflective coating. The Cd, and probably the Cd-Zn targets (composition has not been examined), do not meet the specification established in the Telic purchase order and are believed to be marginal for producing semiconducting coatings. Nevertheless, the quality of the Cd target tubes is believed to be superior in purity (approximately 5-9's) and casting quality (density, grain uniformity, etc.) to the targets (cast at Telic and Haselden Co.) that were used in the preliminary CdS reactive sputtering studies described in Technical Progress Report No. 2. Because of this, and the fact that it is estimated that several weeks will be required before high purity targets can be cast, it was decided that the rejected Cd and Cd - 20 atomic percent Zn target tubes along with the Cd

LOCKHEED PALO ALTO RESEARCH LABORATORY
LOCKHEED MISSILES & SPACE COMPANY, INC.
A SUBSIDIARY OF LOCKHEED AIRCRAFT CORPORATION

end discs should be purchased from Cominco American. These would be used in the interim, so that certain aspects of the $Cd_xZn_{1-x}S$ research could get underway. Sputtering from the end discs is much less than from the tubular section, so that it is believed that the Cd end caps, which are of approximately 4-9's purity, can be used effectively for both the Cd and the Cd-Zn experiments. The Cd target tube and end discs have been received at Telic and installed. The casting quality of the Cominco American parts is indeed superior to that of the previously used targets. Figure 3 shows the Cominco American Cd cathode assembled into a cylindrical magnetron sputtering source.

Additional experiments are underway to explore other casting procedures. In one test a pre-cast 6-9's Cd plate was attached to one of the Ni-plated Cu end discs using an In-Sn eutectic (48 atomic percent Sn, melting point $\sim 120^\circ C$). Good wetting and bonding resulted. However, both In and Sn apparently diffused through the solid Cd and were identified on the free surface. Sectioning of the plate revealed the following. At a point about 20 mil from the Ni surface, 70 ppm In, 50 ppm Sn and 1 ppm Ni were detected. At a point about 1/16" from the Ni surface, 30 ppm In, 50 ppm Sn and 1 ppm Ni were detected. No Cu was detected in any of the experiments. Indium has been considered as a possible donor dopant for the CdS and $Cd_{1-x}Zn_xS$ coatings. Therefore the above procedure could be used with indium as a bonding agent. However, other approaches are also under investigation. Cominco American is conducting experiments to test the use of conducting epoxy (Ag - additive) to attach the precast Cd to the backing support. Direct casting of the Cd onto a stainless steel support, as was done in the original Telic work, is also under investigation. The possibility of making slight modifications to the magnetron design, so that stresses on the Cd are minimized and so that solid Cd or Cd-Zn tubes and end discs might be used, is also under study. It is believed that several of these methods will offer solutions. It will simply be a matter of selecting the most effective approach.

CdS Reactive Sputtering Studies

Reactive sputtering studies are now underway with the magnetron assembly shown in Figure 3 located at the central cathode position shown in Figure 2. The rotatable substrate holder designed for use with the multiple cathode apparatus is located at one (primary) substrate position. An auxiliary substrate holder is located at the second position. Three 1" x 1" Corning 7059 borosilicate glass substrates are mounted in the primary substrate holder. In the experiments currently underway, one plate has predeposited Al diagnostic electrodes as shown in Figure 4. The first series of experiments is being conducted with the primary substrates maintained at a temperature of about 300° C and with various H_2S injection rates at an Ar background pressure of 1 mtorr. The coatings are nominally 10 μm thick. A glass plate coated with indium-tin-oxide is mounted on the auxiliary holder and maintained at 200° C. The object of these tests is to explore the possibility of controlling the coating resistivity through an as-deposited sulfur deficiency. As the work proceeds, other substrate temperatures and argon background pressures will be examined. These studies differ from the preliminary CdS reactive sputtering work described in Technical Progress Report Number 2, in that the emphasis in that work was on achieving stoichiometric coatings.

Two glass cleaning procedures are being used. The first consists of:

1) Trichloroethylene rinse,
2) Isopropyl alcohol rinse,
3) De-ionized water rinse,
4) NH_4OH and de-ionized water soak, brush scrub and soak,
5) De-ionized water rinse,
6) Air dry in clean room.

The second incorporates an HF acid etch of the glass and consists of the following:

1) RT-1 (Chromic acid-sulfuric acid mixture) soak (3 min),
2) De-ionized water rinse,

3) Hydrofluoric acid (16%) etch (30 sec),
4) De-ionized water rinse,
5) NH_4OH and de-ionized water soak, brush scrub, and soak,
6) De-ionized water rinse,
7) Air dry in clean room.

Adhesion and Internal Stress

In the description of the preliminary CdS studies in Technical Progress Report Number 2, it was noted that although good adhesion was consistently achieved on indium-tin-oxide coated substrates, poor adhesion was observed for thick (25 μm) coatings deposited on glass microscope slides by both reactive and direct rf sputtering methods. Poor adhesion was also seen with an aluminum underlay. It is for this reason that the various cleaning procedures and electrode configurations are currently being investigated.

Good adhesion has been found for the CdS coatings deposited on the borosilicate plates during the present series of experiments for both of the cleaning procedures and over both the Al and Nb surfaces. The relative importance of the borosilicate glass, the substrate temperature, and the various cleaning procedures remains to be determined.

Problems of coating adhesion that become more severe with increasing coating thickness can generally be traced to intrinsic stresses within the coating. These stresses result from crystallographic imperfections which are built into the coating during deposition and that are therefore generally constant throughout the coating thickness. Thus a force, which increases with coating thickness, develops at the interface due to the accumulating effect of these stresses. The intrinsic stresses are dependent on the deposition conditions but independent of the substrate material (assuming common substrate surface topography). Measurements of the intrinsic stress can be made by depositing coatings of various thicknesses on thin glass wafer substrates for which the initial state of deflection (due to stresses within the glass) has been determined interferometrically. After deposition the

LOCKHEED PALO ALTO RESEARCH LABORATORY
LOCKHEED MISSILES & SPACE COMPANY, INC.
A SUBSIDIARY OF LOCKHEED AIRCRAFT CORPORATION

incremental change in deflection of the wafers due to the coating is determined by a second interferometric measurement and related to the force per unit width at the interface by assuming elastic behavior of the glass. The slope of a plot of the force per unit width as a function of film thickness provides a measure of the internal stress within the coating. Reactively sputtered CdS coatings in the 500 Å to 3000 Å thickness range are being deposited on stress-measuring wafers, under essentially room temperature conditions. This should constitute a worst case condition for intrinsic stresses since higher substrate temperatures should give a higher degree of crystallographic order. The observed stresses will be compared with the stress levels which have been determined at Telic for a wide range of metallic coatings[1-3].

Substrate Contact (Task 1.3)

Magnetic substrate holders for depositing the upper contact electrodes and the diagnostic electrodes for the semiconductor materials studies have been assembled. Masks for forming diagnostic electrodes with the configuration shown in Figure 4 have been fabricated by an outside vendor using kovar, magnetic stainless steel, and mu-metal sheets of 0.002, 0.003, and 0.005 inch thickness by photo-lithography. An evaluation indicated that the 0.002 and 0.003 inch sheets yielded the best pattern definition, although the various materials performed equally well. A double mask configuration will probably be used for the more demanding upper contact solar cell electrode.

Aluminum diagnostic electrodes deposited on borosilicate substrates cleaned by the first procedure described in the preceding section, or with a chromic acid-sulfuric acid soak, exhibited poor adhesion (did not pass tape test). In subsequent experiments the adhesion was improved somewhat by using a thin reactively sputtered oxide interface between the glass and the aluminum. Excellent adhesion was obtained for aluminum electrodes deposited on glass substrates that had been cleaned in an oxygen glow discharge. The electrodes were 1000 Å thick.

Niobium electrodes were also examined because of the early evidence of poor adhesion of the CdS to aluminum, as discussed in the preceding section.

Niobium diagnostic electrodes and coatings 1000 Å were deposited on glass which had been precleaned by the hydrofluoric acid etch method described in the preceding section. The adhesion of the Nb electrodes and coatings was excellent.

Substrates with the Nb coatings and with the Nb and Al diagnostic electrodes are being used for the CdS reactive sputtered coatings which are currently being deposited. As noted previously, good CdS coating adhesion is being found on all three of the substrates.

Deposition of Cu_2S (Task 1.6)

The first series of Cu_xS reactive sputtering studies has been completed. The coatings were deposited with the copper magnetron sputtering source (shown in Figure 3 of Technical Progress Report Number 2) located in the apparatus configuration shown in Figure 2. The coatings were deposited on 1" x 1" Corning 7059 borosilicate substrates using masks to form the disc pattern, shown in Figure 4.

The coatings were deposited at a rate of about 300 Å/min, with one of the substrates shown in Figure 2 maintained at about 35° C and the other at about 130° C. The substrate temperatures were selected to place one set of substrates above, and the other set below, the transition temperatures for the various copper sulfide phases. The primary deposition variable was the injection rate (partial pressure) of H_2S. Coatings were deposited with H_2S partial pressures ranging from zero to 4 mtorr. The H_2S pumping speed was 100 ℓ/sec. Thus the injection rate was in the range from zero to 0.4 torr-ℓ/sec. Most coatings were deposited with an Ar background pressure of 1 mtorr and were 1500 Å thick. The coatings prepared to date are listed in Table I.

The sputtering target used in this work was fabricated from OFHC copper. A semi-quantitative spectrochemical analysis of thick copper coatings deposited from this cathode yielded in weight percent: Si - 0.0014%, Mg - 0.00064%, Ag - 0.000070%, Ca - 0.00053%, other elements nil, remainder Cu.

The reactively sputtered Cu_xS coatings all yielded good adhesion. However a set of representative Cu_xS coatings in the thickness range from 500 Å to 3000 Å were depositited on glass wafers for coating-internal-stress measurements as described under Task 1.2. Preliminary results indicate that the coatings are in a slight state of tension. Metallic coatings deposited in magnetrons at low pressures are generally in a state of compression[1-3].

Electrical Measurements of Cu_xS (Task 1.8)

The van der Pauw technique was used to determine resistivity, free carrier concentration, and mobility of the Cu_xS films. To overcome the usual difficulties of transport measurements on high resistivity, low mobility samples, the circuit configuration indicated in Figure 5 was used. The JFET input operational amplifiers, LH 0022, provided high impedance, floating connections to three of the sample contacts.

Figure 6 shows the dependence of Cu_xS film resistivity as a function of H_2S partial pressure and substrate temperature. Between 0.75 and 1.0 mtorr of H_2S, the resistivity, ρ_{Cu_xS}, increases five orders of magnitude to 100 Ω-cm. Beyond 1.4 mtorr, the data separate into two catagories; a high resistivity set of films, $\rho \approx 100$ Ω-cm, generally associated with substrate deposition temperature T_s near 130°C, and a low resistivity series of films, $\rho \approx 0.01$ Ω-cm deposited at $T_s \approx 35°C$. Previous investigations of reactively sputtered Cu_xS films had not included the effect of substrate temperature on resistivity[4,5]. The letters A and B in Figure 6 represent high and low resistivity regions at low P_{H_2S}; C and D are the analogous points at high P_{H_2S}. These four representative points are referenced in the following sections.

Hall mobility versus carrier concentration measurements further distinguish these two types of materials as shown in Figure 7. The preponderance of the measured mobility values lies between 1.0 and 6.0 cm^2/V-s and is essentially independent of T_s. The high resistivity films

(10^{16} cm^{-3} < p < 3 x 10^{17} cm^{-3}) exhibit a mobility dependence which is approximately inversely proportional to the carrier concentration; the low resistivity film, (4 x 10^{18} < p < 2 x 10^{20}) have mobility and carrier concentration values which compare well with those of Bugnot et al.[6] also shown in the figure. The functional dependence of the latter data was estimated to be $\mu \alpha p^{-.25}$.

Structural Measurements of Cu_xS (Task 1.7)

To determine the phase(s) present in the 0.15 µm-thick copper sulfide films and to compare the films as a function of the deposition parameter p_{H_2S} for each substrate temperature, x-ray diffraction (XRD), temperature dependence of resistivity (TRD), optical absorption, microprobe and x-ray energy spectroscopy (XES) measurements were performed.

The XRD spectra were obtained for selected films representing regions A, B, C, and D of Figure 6 using a normal incidence x-ray diffractometer with 3 to 4 hours of exposure per film. Results are listed in Table 2. The $Cu_{1.96}S$ phase identified in these films is orthorhombic djurleite and is found by glancing angle XRD to be basal plane oriented. The chalcocite phase is not oriented.

Several of the copper sulfide films were determined to be unstable after repeated or lengthy x-ray exposure during the XRD investigations. Specifically noted were the disappearance of lines used for identification of the chalcocite phase.

The TDR measurements used to supplement XRD phase identification data are summarized by the characteristic signature curves shown in Figure 8. The upper and lower curves represent the resistivity versus temperature behavior of all the high and low resistivity flims, respectively. Phase transition temperatures, as indicated by the breakpoints on the heating leg of the high resistivity curve for samples between A and C, are typically between 103° and 106° C. These are typical of orthorhombic to hexagonal phase

LOCKHEED PALO ALTO RESEARCH LABORATORY
LOCKHEED MISSILES & SPACE COMPANY, INC.
A SUBSIDIARY OF LOCKHEED AIRCRAFT CORPORATION

change temperatures, reported for crystalline high resistivity Cu_2S[7]. Breakpoint temperatures, upon heating for low resistivity film samples of between 96° and 101°C, compare well with orthorhombic to metastable phase change temperatures reported for crystalline low resistivity Cu_2S.

Electron microprobe analysis was performed over several 200 μm diameter areas of selected high and low resitivity films. Ignoring sample-holder-induced edge effects, each film was found to be quite homogeneous in copper to sulfur ratio across its 1 in. diameter. Films along curve AC in Figure 6 (high ρ) contained relatively more copper than those along BD (low ρ). The ratio of Cu/S decreases as p_{H_2S} increases along both AC and BD.

Scanning electron microscopy (SEM) was used for film surface topography investigations. Two series of SEM photographs are shown in Figure 9; again, the high ρ material (upper row of photos) and low ρ material (lower row) are represented and appear from left to right in order of increasing p_{H_2S}. The left-most photo in each row shows the surface of films deposited at $p_{H_2S} \leq 1.0$ μm. The 0.1 to 3 μm diameter nodules evident in the high ρ films were analyzed using XES and found to contain large amounts of Cu compared to that in the nodule-free regions of the same film or to that in the nodule-free film. It is interesting to note that the nodule-free film in the center of the lower row in Figure 9 was deposited at the higher substrate temperature and thus it seems that nodules are connected with high resistivity and not necessarily with high T_s. Also, the nodule density decreases as p_{H_2S} is increased, as also observed by Hsieh[5].

The optical absorption coefficient has been shown to depend on the various Cu_xS phases[8] and so provides another technique for Cu_xS phase identification. The absorption coefficient and refractive index of reactive sputtered Cu_xS films were determined from transmission, $T(\lambda)$, and reflection, $R(\lambda)$, spectra. The $T(\lambda)$ and $R(\lambda)$ shown in Figure 10 is for Cu_xS sample #30 (Table 1). The refractive index may be obtained to first order from the spectral position of reflection maxima and minima. Five extrema of $R(\lambda)$

LOCKHEED PALO ALTO RESEARCH LABORATORY
LOCKHEED MISSILES & SPACE COMPANY, INC.
A SUBSIDIARY OF LOCKHEED AIRCRAFT CORPORATION

from Figure 10 were used to derive an approximation to the index of refraction:

$$n_1(\lambda) \approx 4.175 - \lambda(\mu m) \tag{1}$$

over the spectral range $0.4 \leq \lambda \leq 1.8$ μm. The approximation of Eq. (1) is compared with the refractive index for principal axis polarizations reported for single crystal chalcocite[9] in Figure 11.

To derive the optical constants of a film from $T(\lambda)$ and $R(\lambda)$ measurements, it may be more convenient to work with the functions $\frac{1+R}{T}$ and $\frac{1-R}{T}$ as suggested by Tomlin[10]. In particular, when the absorption coefficient, α, satisfies the inequality

$$\frac{\alpha d}{4\pi} \ll n_1 \quad ,$$

the approximate relation

$$\frac{1-R}{T} \approx \frac{1}{4n_1n_2} \left[(n_1 + n_2)^2 e^{\alpha d} - (n_1 - n_2)^2 e^{-\alpha d}\right] \tag{2}$$

is obtained from Tomlin's Eq.(5)[10] where n_2 is the refractive index of the glass substrate, $n_2 = 1.5$. The solution of Eq. (2)

$$\alpha = \frac{1}{d} \ln \left\{\frac{1-R}{T} \frac{2n_1n_2}{(n_1 + n_2)^2} \left[1 + \sqrt{1 + \left(\frac{T}{1-R}\right)^2 \frac{(n_1 - n_2)^2 (n_1 + n_2)^2}{4n_1^2 n_2^2}}\right]\right\} \tag{3}$$

is not a sensitive function of n_1 or n_2. In particular, interference effects cancel out to first order in the function $\frac{1-R}{T}$, resulting in the simple form of Eq. (2).

The absorption coefficient derived from the data of Figure 10 and Eq. (3) is shown in Figure 12. (The absorption coefficient of a film is obtained from the average,

$$\bar{\alpha} = \frac{1}{3}\alpha_{\parallel} + \frac{2}{3}\alpha_{\perp}$$

of absorption coefficients of the principal axes polarizations measured on a

LOCKHEED PALO ALTO RESEARCH LABORATORY
LOCKHEED MISSILES & SPACE COMPANY, INC.
A SUBSIDIARY OF LOCKHEED AIRCRAFT CORPORATION

single crystal.) It is clear that the dominant component of Cu_xS film absorption in Figures 10 or 12 is due to the chacocite phase of Cu_xS.

In Figure 13 we show the absorption coefficients of a number of films deposited under various conditions. From the absorption edge at $\lambda \approx 0.95$ µm, it appears that films #17 and #8 also contain a significant fraction of the chalcocite phase. The rather flat absorption for $\lambda \gtrsim 1.0$ µm is probably due to shadowing by Cu rich nodules in the film. For film #8, an apparent absorption coefficient $\alpha \approx 8 \times 10^3$ cm^{-1} corresponds to 12% of the film surface covered with opaque nodules. This is consistent with the corresponding SEM photograph in Figure 9. For film #17, $\alpha \approx 2.5 \times 10^3$ cm^{-1} corresponds to 4% of the film surface being covered by nodules. Again, the result is consistent with the SEM photo (not shown). Film #20 is free from Cu nodules (Figure 9) but exhibits a significant free carrier absorption consistent with that of djurleite (Figure 12) and the XRD identification (Table 2).

SUMMARY

By cylindrical-post magnetron reactive sputtering one can deposit thin films of chalcocite phase copper sulfide. Also, by adjustments in deposition parameters, principally reactive gas pressure P_{H_2S} and substrate temperature T_S, the stoichiometry of the films can be varied over the range of interest important to the application of this process to manufacture of low cost heterojunction solar cells.

In this work, we have shown that two types of Cu_xS films, i.e., high resistivity and low resistivity, can be deposited on glass substrates using T_S as the primary control parameter. Generally the high resistivity films contain Cu-rich nodules which appear to be growing out of the film.

Before drawing two further conclusions, we note that Okamoto and Kawai[7] found resistivities on the order of 100 Ω cm in near stoichiometric Cu_xS when the crystals contained Cu precipitates. The excess Cu was introduced

by either excess Cu introduced during Bridgman growth or by Cu diffusion into extant crystals. Chalcocite crystals without excess Cu displayed resistivities 3 orders of magnitude lower. The conclusions to be drawn are that (1) chalcocite films may be deposited with transport properties similar to Bridgman grown crystals, and (2) excess Cu is necessary to compensate acceptor-type native defects (presumably Cu vacancies in near stoichiometric chalcocite).

ANTICIPATED ACTIVITIES DURING NEXT REPORTING PERIOD

- Task 1.1: The multi-cathode assembly will be installed in the chamber that is dedicated to the program, and shakedown tests will be completed.

- Task 1.2: The CdS reactive sputtering studies to deposit coatings with controlled resistivity will be completed using the 5-9's target. These studies will be followed by a shakedown of the multi-cathode system, as described in Task 1.1 above. At this point the $Cd_{1-x}Zn_xS$ 6-9's targets should be available. The reactive sputtering studies to deposit coatings with the desired resistivity and grain size will then be continued using these targets. The primary deposition parameters will be the H_2S injection rate and the substrate temperature. The influence of the Ar background pressure will also be examined.

- Task 1.3: CdS/Al and $Cd_{1-x}Zn_xS$/Al contact fabrication details will be worked out during the course of the work described in Task 1.2 above. In particular, the conditions required to establish ohmic contact between the metallization and semiconductor film will be established.

- Task 1.4: Structural measurements of $Cd_xZn_{1-x}S$ films will be made as a function of deposition conditions and post-deposition heat treatments.

- Task 1.5: Electrical and optical properties of $Cd_xZn_{1-x}S$ films will be measured as a function of deposition conditions and post-deposition heat treatment. In particular, the necessary heat treatment required for conductivity control in each alloy will be established.

- Task 1.9: The first CdS/Cu_2S junctions will be formed and evaluated.
- Task 2.2: The masks for use in depositing the Au top grid electrodes will be fabricated and tested by depositing Cu grid structures on glass substrates. SEM analysis will be used to evaluate the geometry and structure of the resulting grids.

LOCKHEED PALO ALTO RESEARCH LABORATORY
LOCKHEED MISSILES & SPACE COMPANY, INC.
A SUBSIDIARY OF LOCKHEED AIRCRAFT CORPORATION

REFERENCES

1) D. W. Hoffman and J. A. Thornton, "Internal Stresses in Sputtered Chromium," Thin Solid Films, 40, 355 (1977)

2) J. A. Thornton and D. W. Hoffman, "Internal Stresses in Titanium, Nickel, Molybdenium, and Tantalum Films Deposited by Cylindrical Magnetron Sputtering." J. Vac. Sci. Technol., 14, 164 (1977)

3) D. W. Hoffman and J. A. Thornton, "The Compressive Stress Transition in Al, V, Zr, Nb, and W Films Sputtered at Low Working Pressures," Thin Solid Films, 45, 387 (1977)

4) Technical Progress Report No. 2, Cadmium Sulfide/Copper Sulfide Heterojunction Cell Research, Lockheed Missiles & Space Company, LMSC-D623523 (31 March 1978)

5) E. J. Hsieh, Proceedings of the Photovoltaics Program Semi-Annual Review, Advanced Materials R&D Branch, Golden, CO, 315 (4-6 October 1977)

6) J. Bugnot, F. Gustavino, S. Couve-Duchemin, and M. Savelli, Proceedings International Workshop - Cadmium Sulfide Solar Cells and Other Abrupt Heterojunctions, U of Delaware, 327 (1975)

7) K. Okamoto and S. Kawai, Jap. JAP., 12, 1130, (August 1973)

8) B. J. Mulder, Phys. Stat. Sol. (a) 13, 79 (1972)

9) B. J. Mulder, Phys. Stat. Sol. (a) 15, 409 (1973)

10) S. G. Tomlin, Brit. J. Appl. Phys. (J. Phys. D), ser 2 1, 1667 (1968)

TABLE 1

REACTIVE SPUTTERED COPPER SULFIDE COATINGS

Sample Number	Telic Ref.	Ar Pres. (mTorr)	H_2S Pres. (mTorr)	Temperature	Thickness
1	3-36	1.0	0.75	120°C	1500 Å
2	"	"	"	100°C	"
3	"	"	"	30°C	"
4	3-41	1.5	1.0	100°C	"
5	"	"	"	30°C	"
6	3-46	1.5	1.40	100°C	"
7	"	"	"	50°C	"
8	3-50	1.5	1.13	30°C	"
9	3-55	2.0	1.06	100°C	"
10	"	"	"	30°C	"
11	3-58	2.0	2.0	100°C	"
12	"	"	"	45°C	"
13	3-62	2.0	1.70	130°C	"
14	"	"	"	42°C	"
15	3-66	2.0	3.0	130°C	"
16	"	"	"	42°C	"
17	3-72	2.0	2.5	130°C	"
18	"	"	"	40°C	"
19	3-76	2.0	4.0	130°C	"
20	"	"	"	35°C	"
21	3-80	2.0	1.50	130°C	"
22	"	"	"	40°C	"
23	3-84	2.0	1.0	130°C	"
24	"	"	"	35°C	"
25	3-87	2.0	0	130°C	"
26	"	"	"	35°C	"
27	3-90	5.0	1.50	130°C	"
28	"	"	"	35°C	"
29	3-94	2.0	1.60	130°C	"
30	"	"	"	35°C	"

Sample Number	Telic Ref.	Ar Pres. (mTorr)	H_2S Pres. (mTorr)	Temperature	Thickness
31	3-98	2.0	1.40	130°C	1500 Å
32	"	"	"	35°C	"
33	3-102	2.0	1.80	130°C	"
34	"	"	"	35°C	"
35	3-106	2.0	2.25	130°C	"
36	"	"	"	35°C	"
41	4-23	2.0	4.0	200°C	"
42	"	"	"	80°C	"
43	4-25	2.0	1.75	200°C	"
44	"	"	"	80°C	"
45	4-27	2.0	1.25	130°C	"
46	"	"	"	45°C	"
47	4-30	2.0	4.0	130°C	10,000 Å
48	"	"	"	40°C	"
49	4-36	2.0	4.0	200°C	1500 Å
50	"	"	"	80°C	"
51	4-38	2.0	1.75	200°C	"
52	"	"	"	80°C	"

TABLE 2

XRD RESULTS

Figure 6 Region	Identified Majority Phase	Identified Minority Phase
A	Cu_2S	$Cu_{1.96}S$
B	$Cu_{1.96}S$	
C	$Cu_{1.96}S$	Cu_2S
D	$Cu_{1.96}S$	

FIGURE CAPTIONS

1) Specialized deposition system consisting of four cylindrical magnetron sputtering sources and rotatable substrate holder in common vacuum chamber.

2) Coating chamber with single central post magnetron sputtering source.

3) Cadmium sputtering source for specialized deposition system.

4) Sputter mask and contact configuration for van der Pauw measurements on semiconducting films.

5) Van der Pauw measuring circuit for use with high impedance samples.

6) Effect of substrate temperature and H_2S partial pressure on resistivity of Cu_xS films.

7) Hall mobility versus carrier concentration for Cu_xS films.

8) Temperature dependence of resistivity for Cu_xS films. Arrowheads denote direction of thermal cycling.

9) SEM photographs of Cu_xS films at 5000 x.

10) Transmission and reflection spectra of Cu_xS film with large chacocite component.

11) Comparison of Cu_xS film refractive index and single crystal chalcocite principal axis refractive indices from reference [9].

12) Absorption coefficient of Cu_xS film No. 30 compared to absorption coefficient of various Cu_xS phases.

13) Absorption coefficient of several Cu_xS films showing specific identifiable features (see text).

LOCKHEED PALO ALTO RESEARCH LABORATORY
LOCKHEED MISSILES & SPACE COMPANY, INC.
A SUBSIDIARY OF LOCKHEED AIRCRAFT CORPORATION

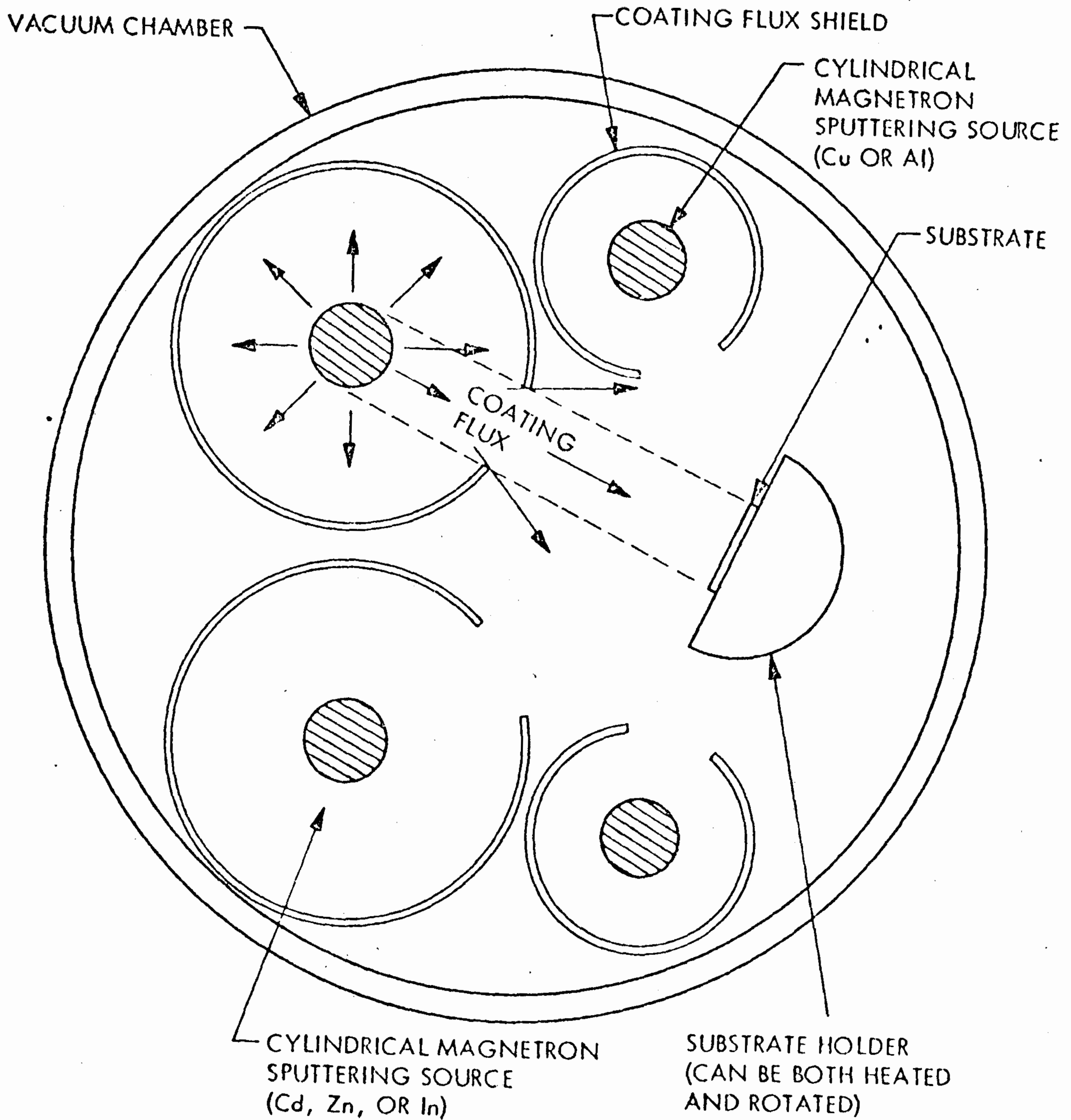

Fig. 1 Specialized deposition system consisting of four cylindrical magnetron sputtering sources and rotatable substrate holder in common vacuum chamber.

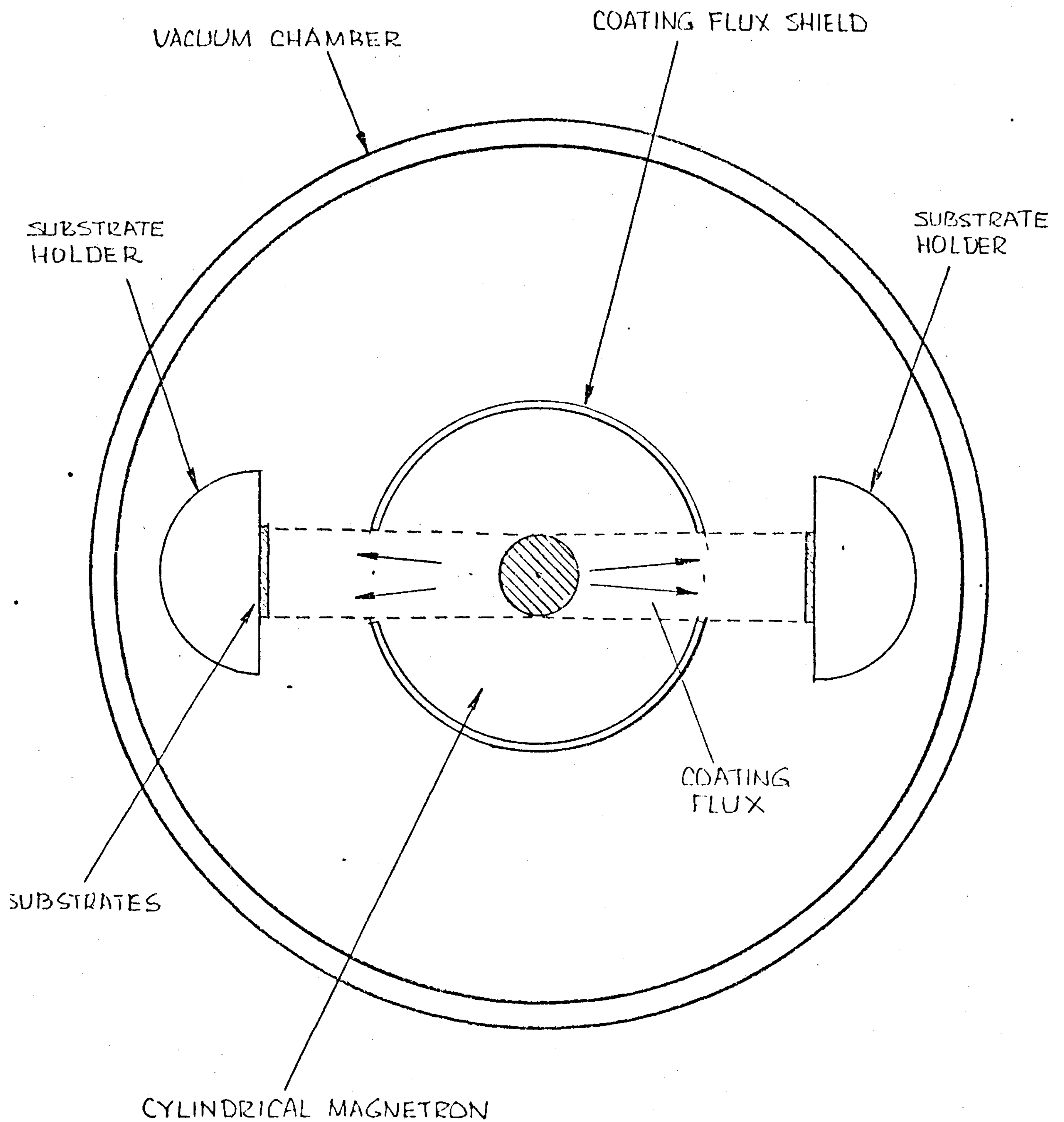

Fig. 2 Coating chamber with single central post magnetron sputtering source.

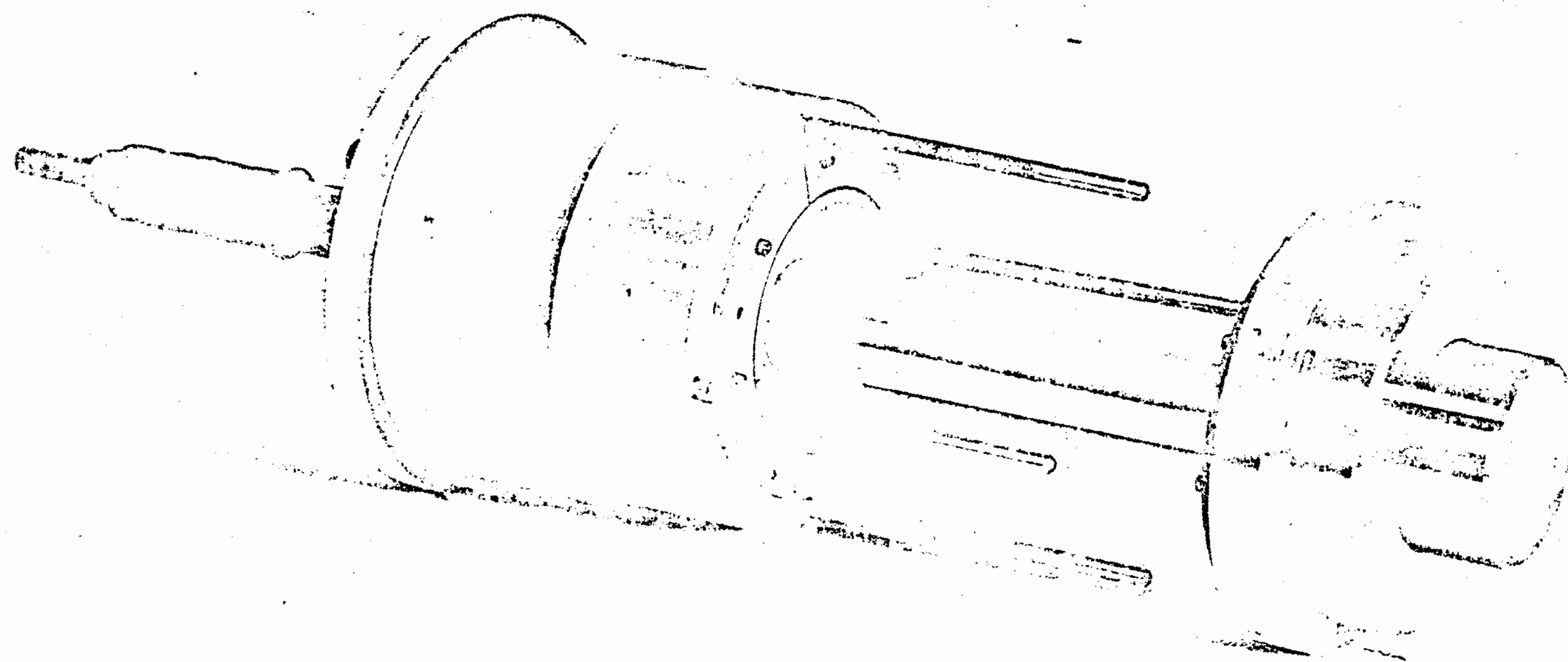

Fig. 3 Cadmium sputtering source for specialized deposition system.

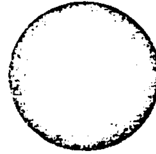

a. $Cd_{1-x}Zn_x$ and Cu_2S deposition pattern

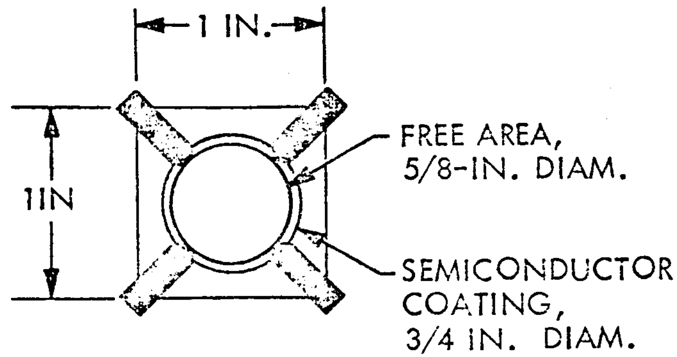

b. Substrate contact metallization pattern

Fig. 4 Sputter mask and contact configuration for van der Pauw measurements on semiconducting films.

LOCKHEED PALO ALTO RESEARCH LABORATORY
LOCKHEED MISSILES & SPACE COMPANY, INC.
A SUBSIDIARY OF LOCKHEED AIRCRAFT CORPORATION

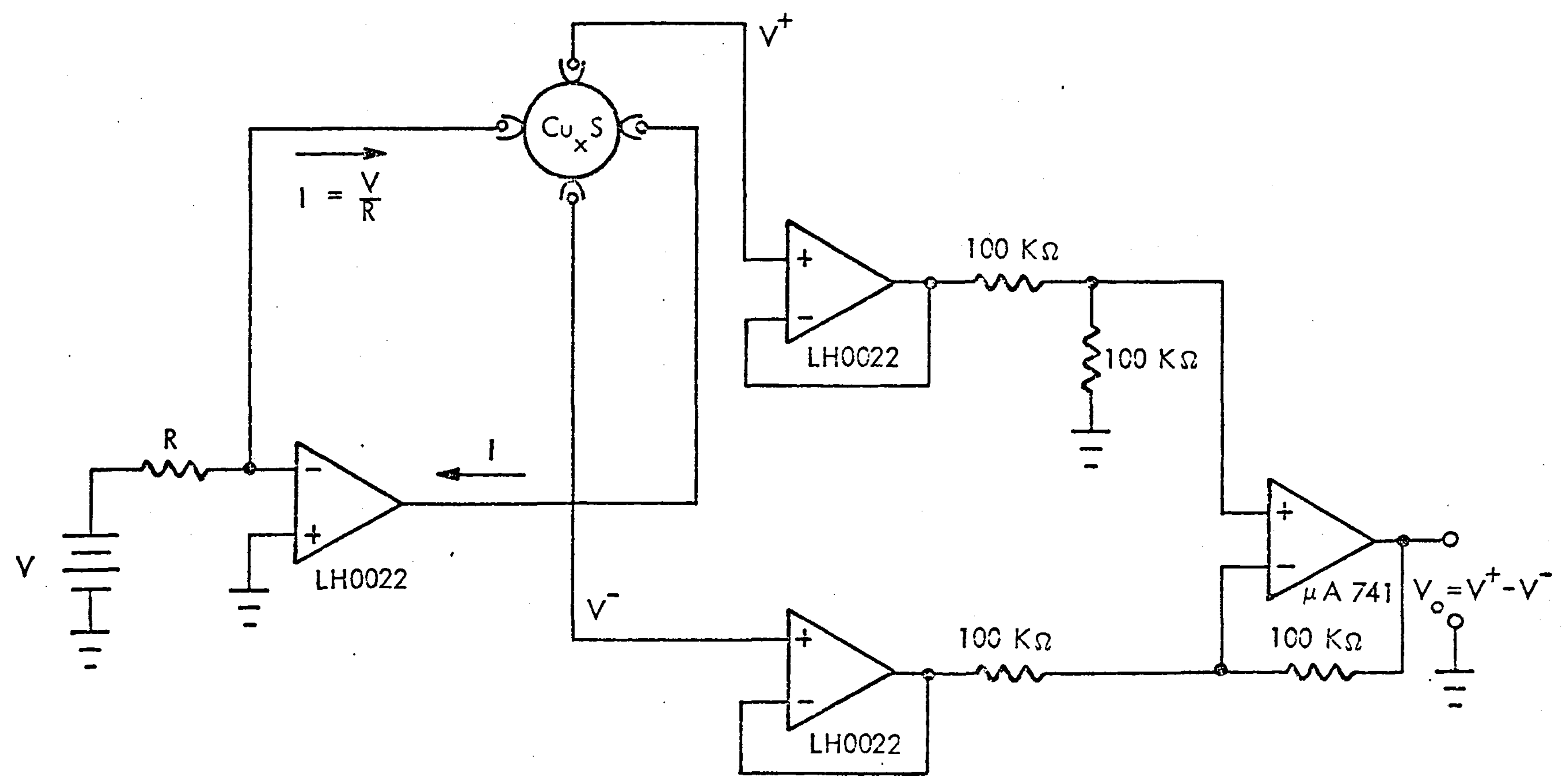

Fig. 5 Van der Pauw measuring circuit for use with high impedance samples.

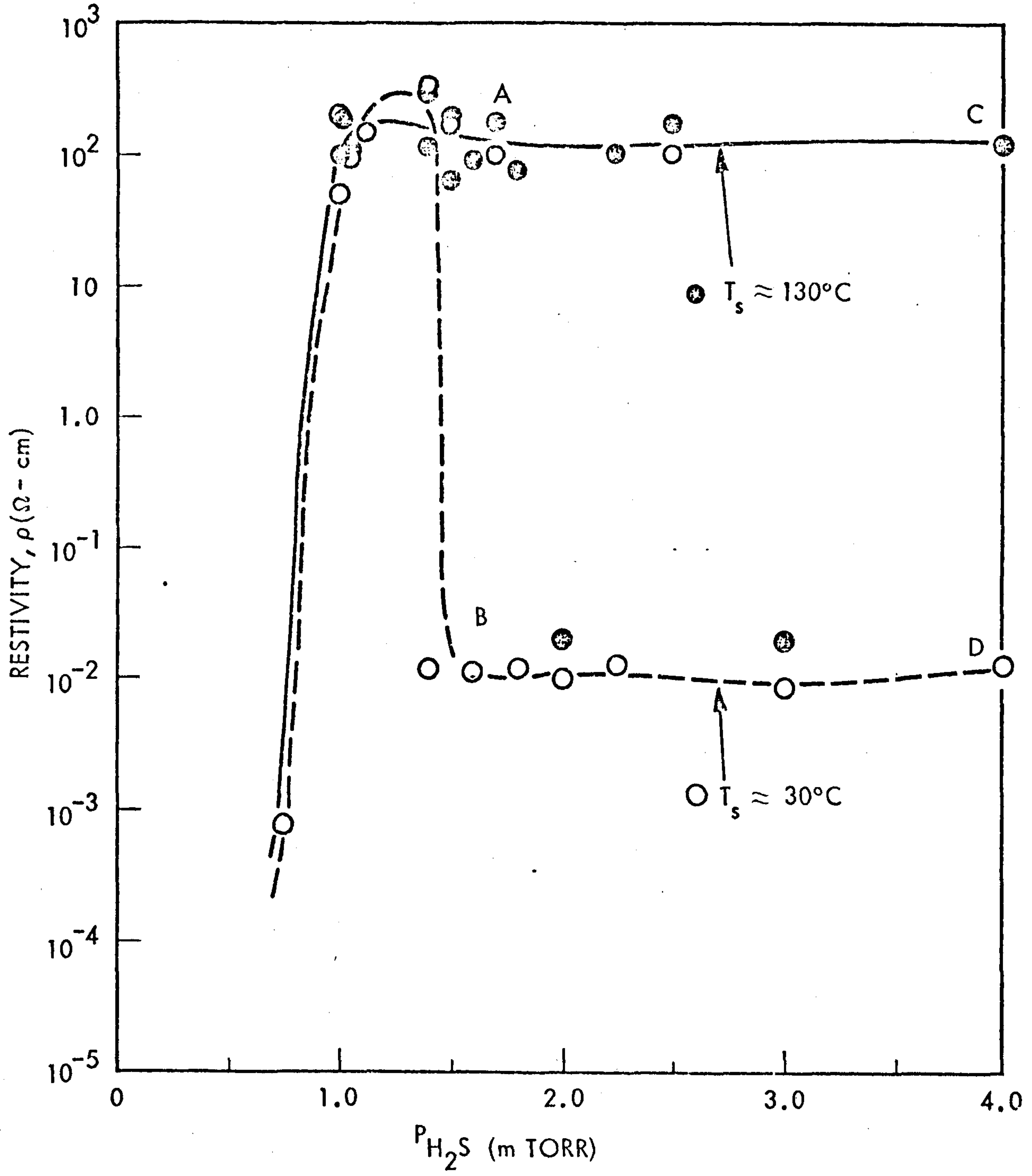

Fig. 6 Effect of substrate temperature and H_2S partial pressure on resistivity of Cu_xS films.

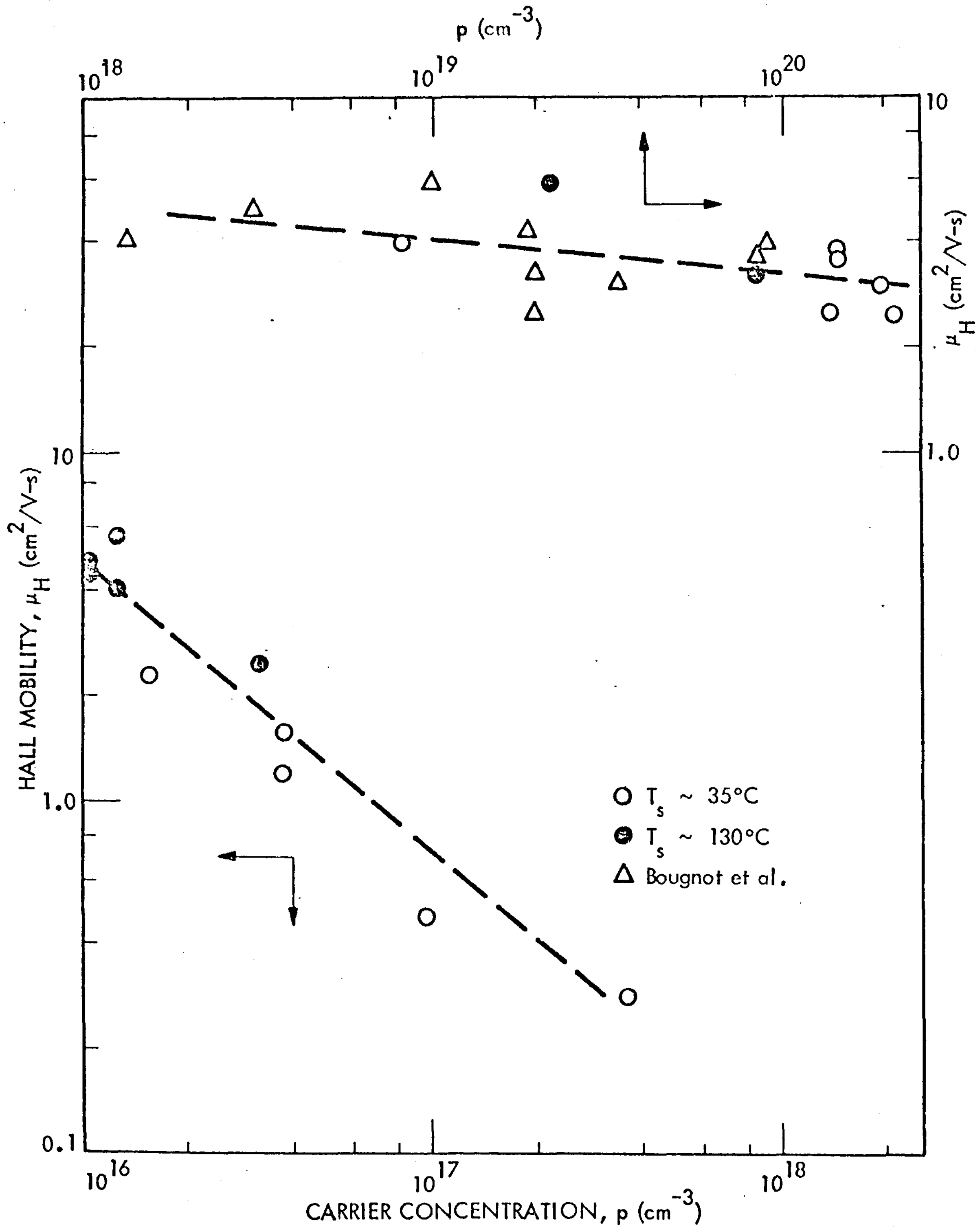

Fig. 7 Hall mobility versus carrier concentration for Cu_xS films.

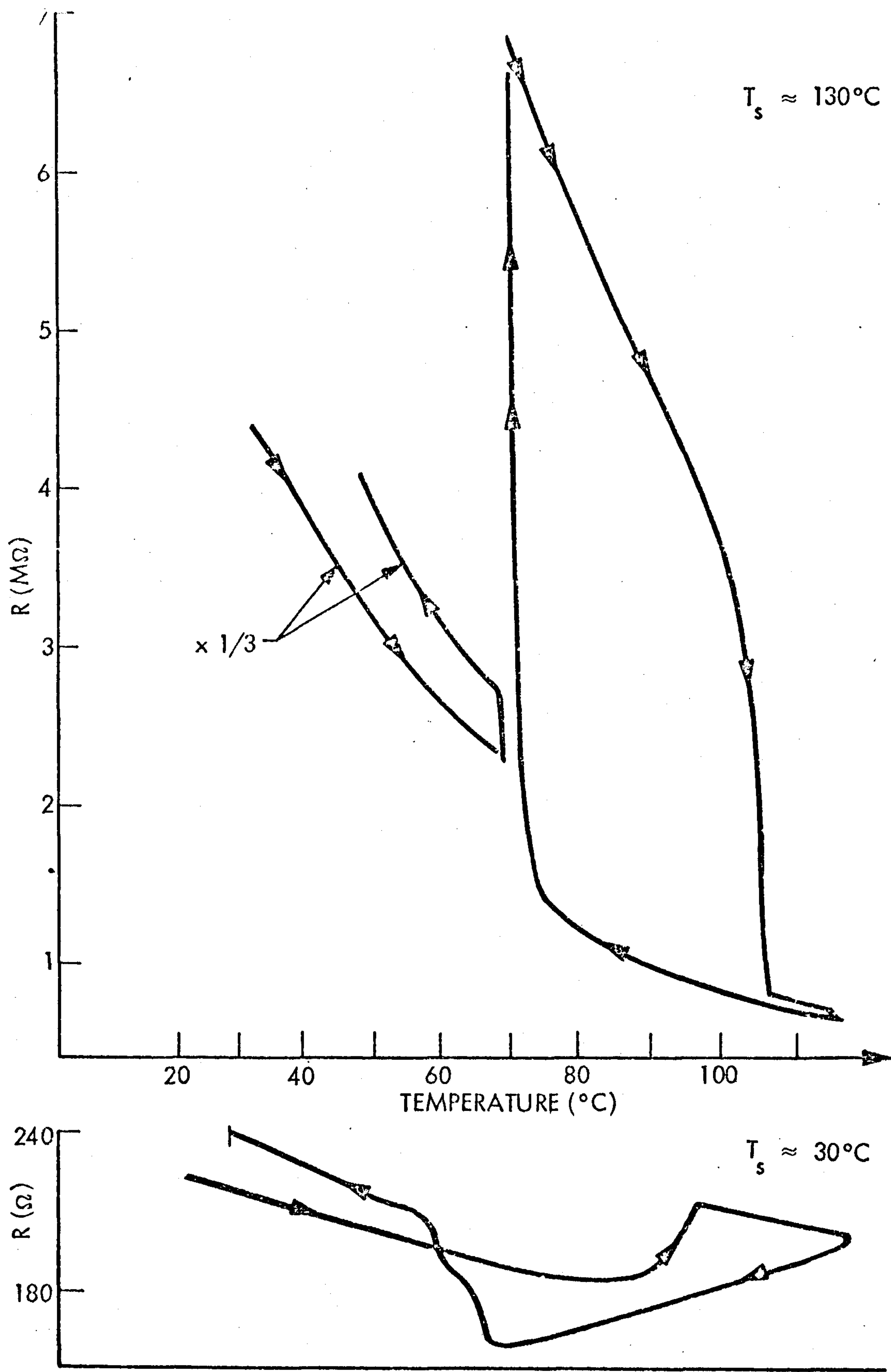

Fig. 8 Temperature dependence of resistivity for Cu_xS films. Arrowheads denote direction of thermal cycling.

No. 4: 1.0 μm,(a) 100°C (b)

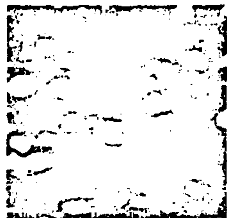

No. 8: 1.125μm, 30°C

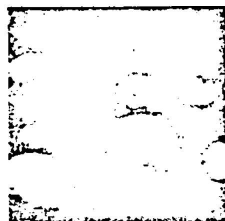

No. 6: 1.4 μm, 100°C

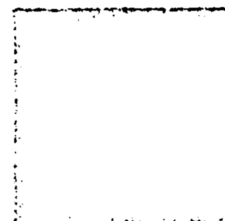

No. 35: 2.25 μm, 130°C

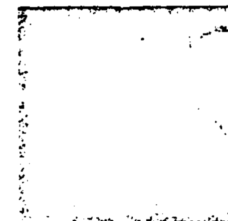

No. 19: 4 μm, 130°C

No. 3: 0.75 μm, 30°C

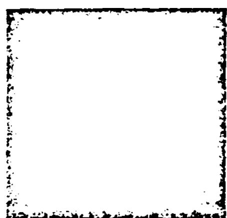

No. 32: 1.4 μm, 35°C

No. 11: 2.0 μm, 100°C

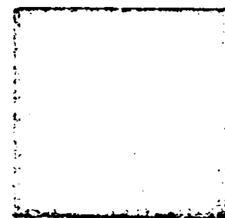

No. 36: 2.25 μm, 35°C

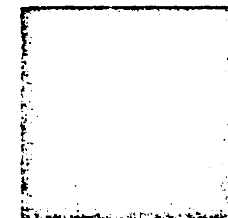

No. 20: 4.0 μm, 35°C

(a) P_{H_2S} in μm.

(b) T_S in °C

Fig. 9 SEM photographs of Cu_x films at 5000x.

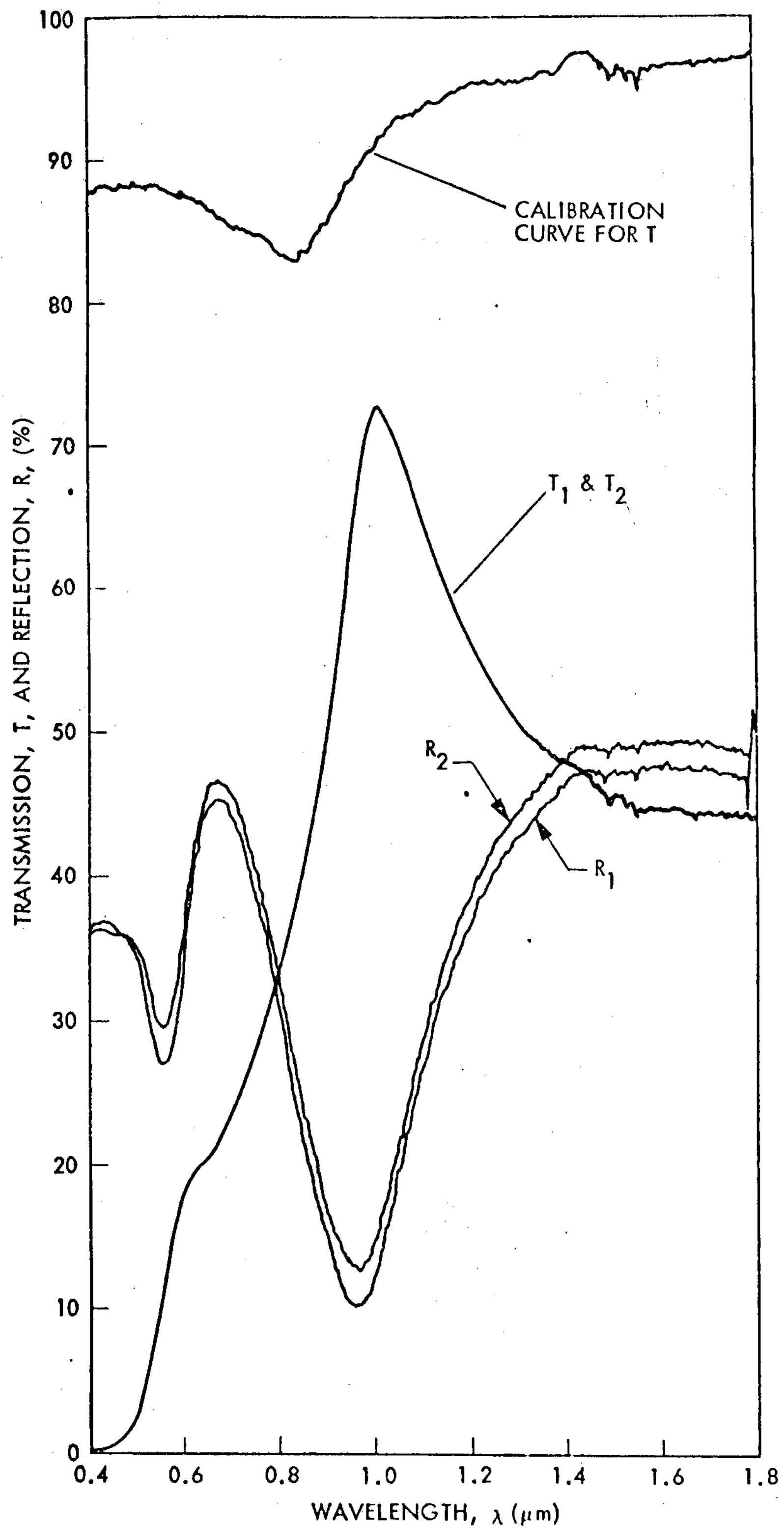

Fig. 10 Transmission and reflection spectra of Cu_xS film with large chacocite component.

LOCKHEED PALO ALTO RESEARCH LABORATORY
LOCKHEED MISSILES & SPACE COMPANY, INC.
A SUBSIDIARY OF LOCKHEED AIRCRAFT CORPORATION

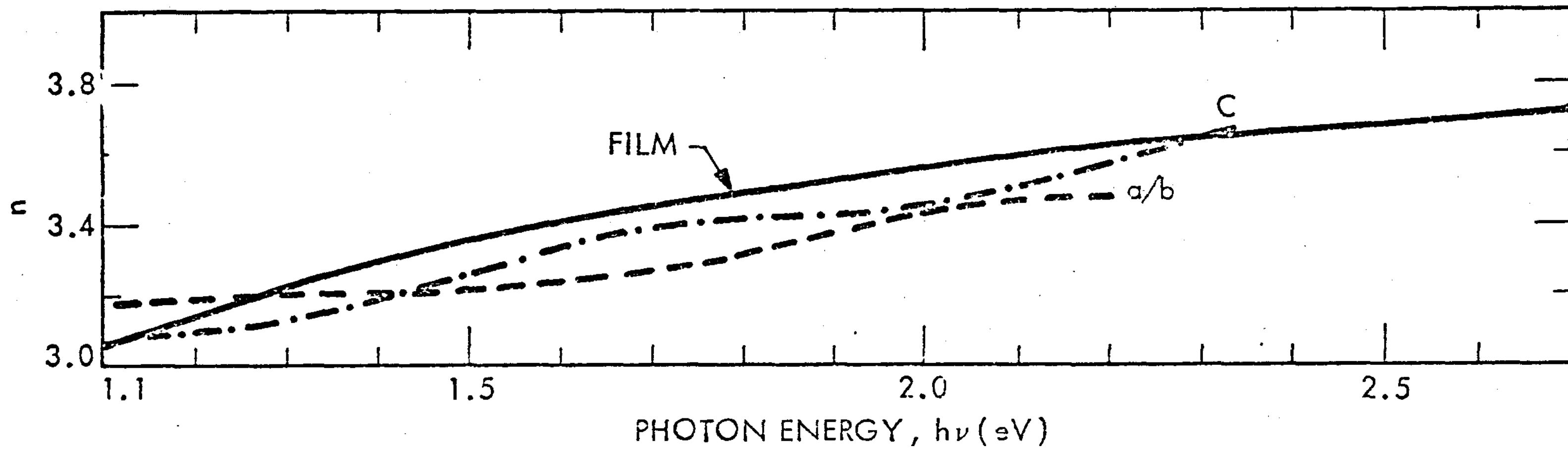

Fig. 11 Comparison of Cu_xS film refractive index and single crystal chalcocite principal axis refractive indices from reference [9].

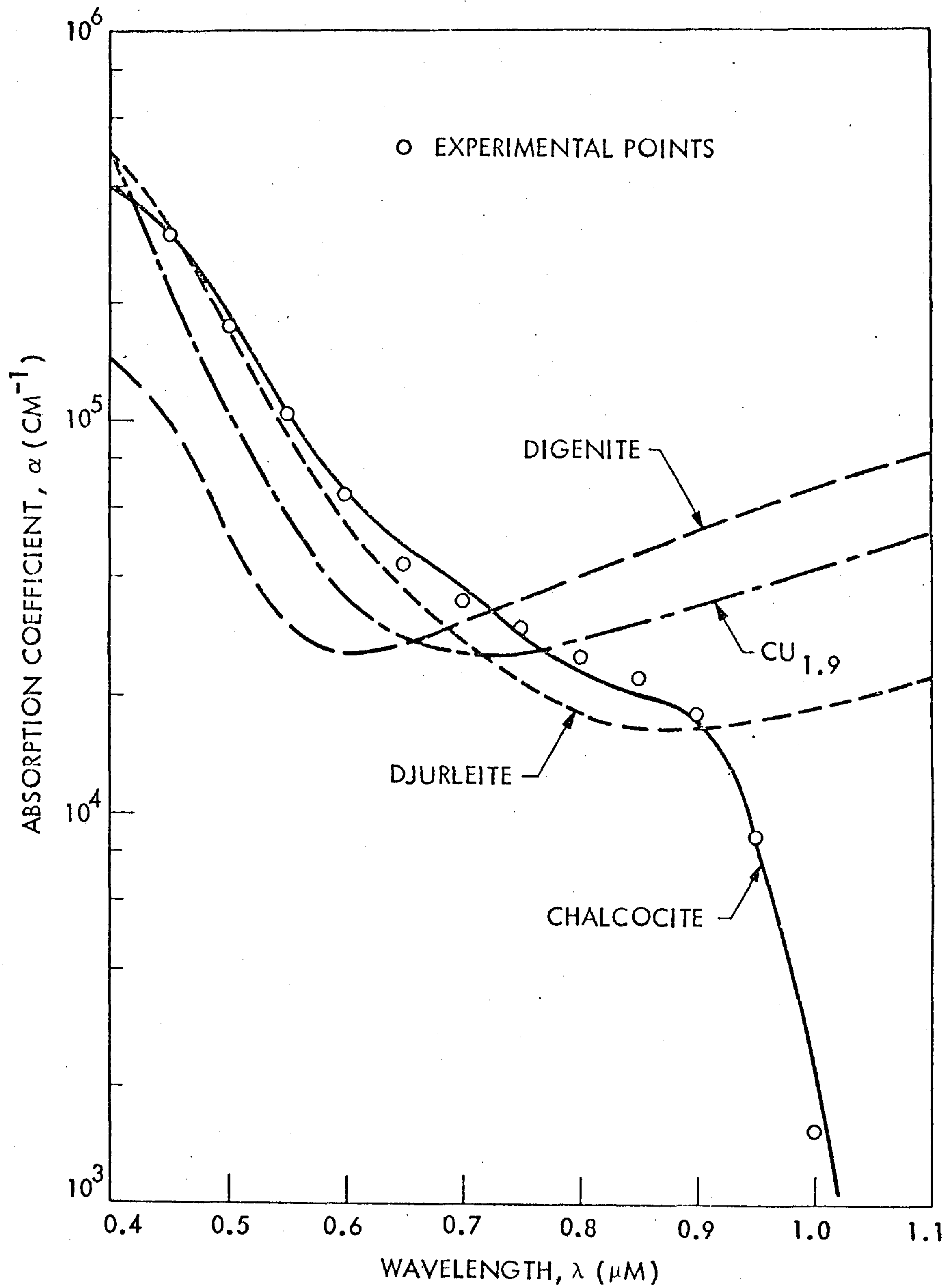

Fig. 12 Absorption coefficient of Cu_xS film No. 30 compared to absorption coefficient of various Cu_xS phases.

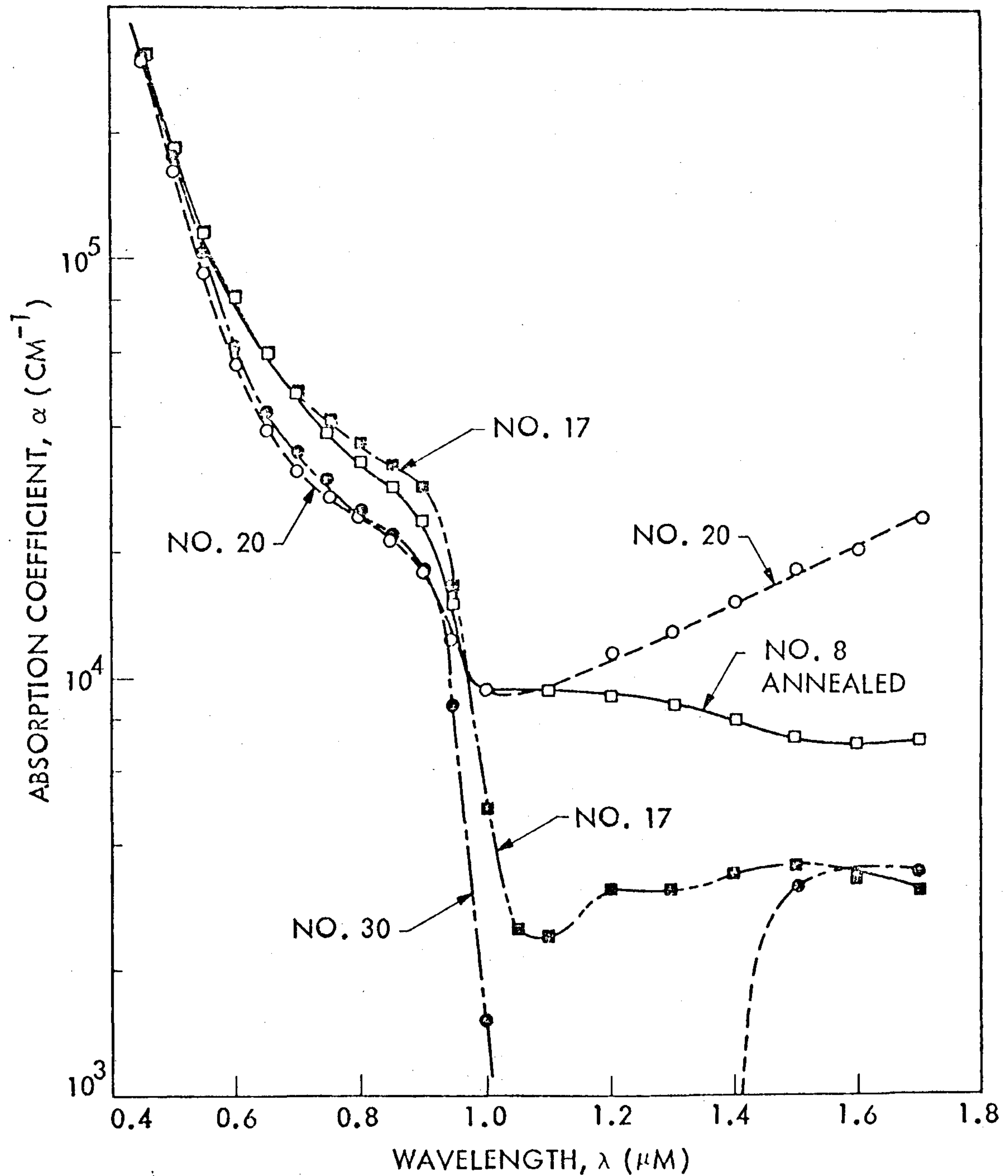

Fig. 13 Absorption coefficient of several Cu_xS films showing specific identifiable features (see text).